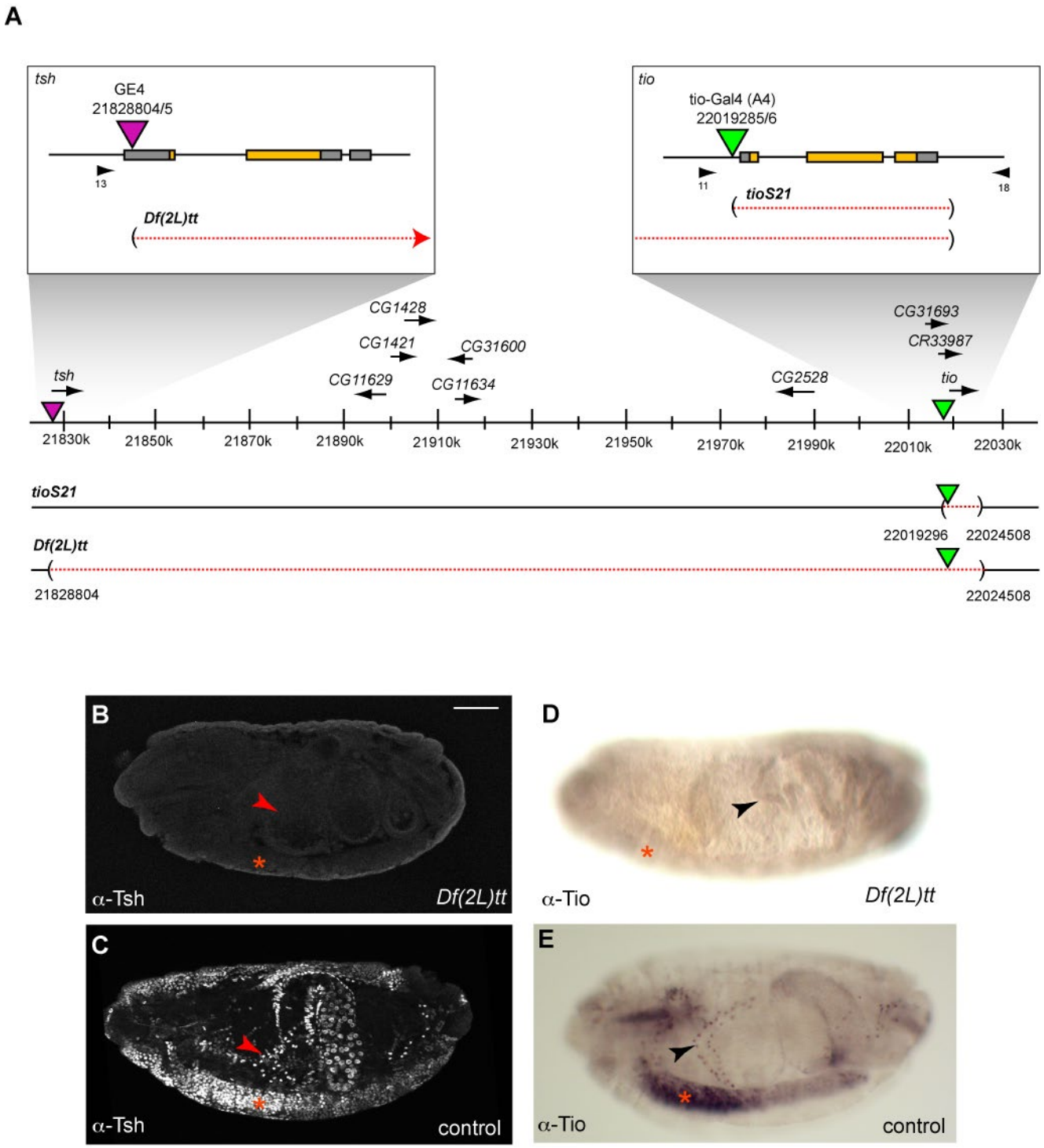

Fig. S1. Molecular mapping of the *tsh-tio* and *tio* deficiency lines. (**A**) The *tsh-tio* genomic locus spans cytological positions 40A5 to 40D3 and is ~200 kb in length. The centromere is on the right. More detailed views of the *tsh* and *tio* loci are illustrated in the upper boxes and show intron-exon structure, coding sequence (yellow) and extent of the genomic deficiencies (red dashed lines between brackets). There are seven predicted but uncharacterised protein-coding genes and one non-protein coding gene (*CR33987*) between *tsh* and *tio* (arrows). The P-element insertions used to generate the deficiencies are shown as triangles (*tsh*, purple and *tio*, green) and their genomic insertion points are given. The insertion in *tio* has been described previously by Tang and Sun (Tang and Sun, 2002) , where it is referred to as *tioA4*. The insert in *tsh* (*GE4*) was generated as part of this study. *tioS21* and *Df(2L)tt* are depicted below, with the extent of the genomic deficiency indicated by the broken red line between brackets. Primer sets 13+18 and 11+18 (arrowheads) were used to amplify across the deficiencies for sequencing. A region of the P-element remained after excision of *tio-Gal4(A4)* and is present in *tioS21* and *Df(2L)tt* deficiency lines. *tioS21* removes *tio* and part of the overlapping gene *CR33987*. *Df(2L)tt* removes all genes between and inclusive of *tsh* and *tio*. *tios21* is a protein null for Tio (data not shown). (**B-E**) *Df(2L)tt* is a protein null for Tsh and Tio. Tsh (B,C) and Tio (D,E) expression in *Df(2L)tt* (B,D) and sibling control (C,E) embryos. Arrowheads indicate anterior MpT and asterisk indicates staining in the central nervous system. Scale bars: 50 μm.

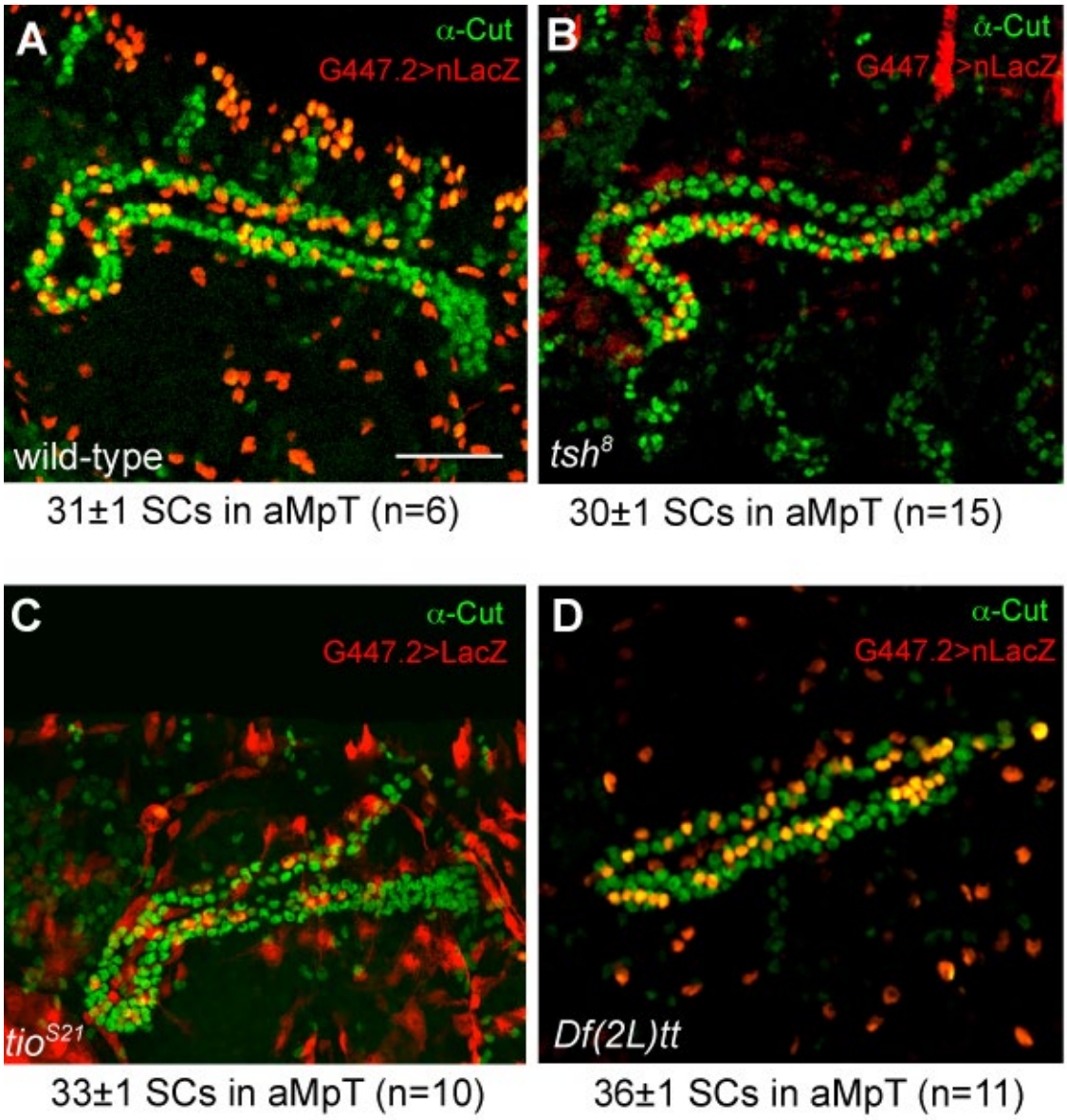

Fig. S2. Tsh and Tio show little or no morphological MpT defects in embryos. (A-D) Stage 16 embryonic MpTs stained for Cut (green) and the SC-marker G447.2>*lac*Z (red). SCs are present with approximately the normal number and normal spacing in *tsh* (**B**) and *tio* (**C**) single mutants and *tsh tio* double mutants (**D**), compared with wild-type (**A**). SC numbers for each genotype are given. Scale bars: 50 μm.

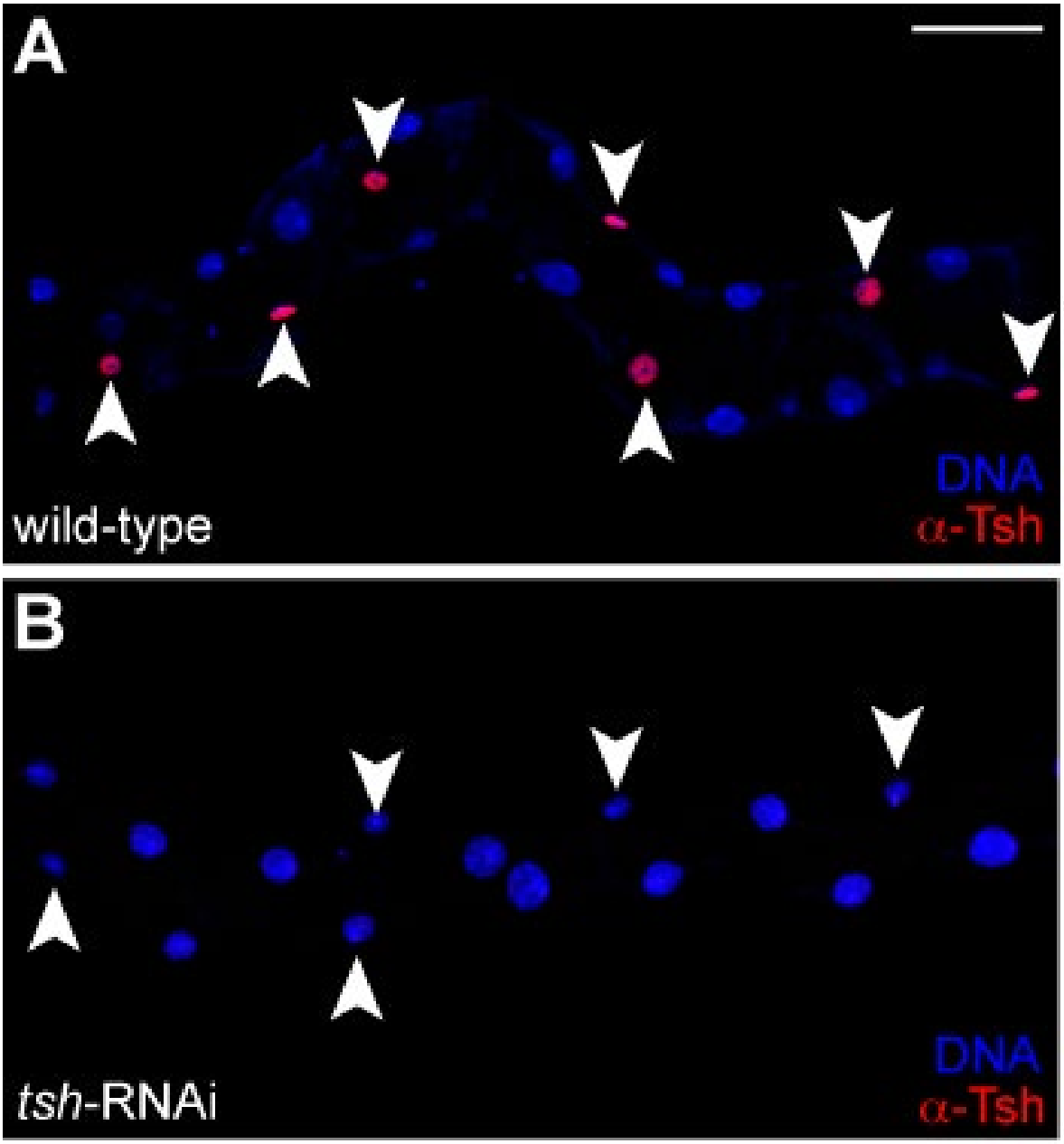

Fig. S3. Effective Tsh knockdown by RNAi. (A,B) Adult Malpighian tubules stained for Tsh (red) and DNA (blue). Arrowheads indicate SCs (identified by their small nuclear size compared to PCs). (**A**) Wild-type tubule, Tsh is expressed in all SCs. (**B**) *c724>UAS-tsh-RNAi*, Tsh expression is abolished in SCs after RNAi knockdown (a total of 38 *c724>UAS-tsh-RNAi* tubules were examined, corresponding to over 1000 SCs). Scale bars: 30 μm.

Table S1. The 20 most downregulated genes in E14.5 *Tshz3* mutant ureters

	Fold change (KO versus WT)	**Gene symbol**	**Gene title**
10583809	−2.953	Cnn1	calponin 1
10437885	−2.748	Myh11	myosin, heavy polypeptide 11, smooth muscle
10545707	−2.531	Actg2	actin, gamma 2, smooth muscle (Smaa)
10386996	−2.476	Myocd	myocardin
10579054	−2.160	4930467E23Rik	RIKEN cDNA 4930467E23 gene
10538459	−2.158	Aqp1	aquaporin 1
10528177	−2.129	Speer4e	spermatogenesis associated glutamate (E)-rich protein
10603232	−2.118	Gmcl1l	germ cell-less homolog 1 (Drosophila)-like
10467124	−2.114	Acta2	actin, alpha 2, smooth muscle
10350630	−2.081	Fam129a	family with sequence similarity 129, member A
10571601	−2.053	Pdlim3	PDZ and LIM domain 3
10577388	−2.007	4930467E23Rik	RIKEN cDNA 4930467E23 gene
10528183	−2.004	Speer4e	spermatogenesis associated glutamate (E)-rich protein
10345101	−1.895	Col9a1	collagen, type IX, alpha 1
10578045	−1.883	Nrg1	// neuregulin 1
10599673	−1.866	4930527E24Rik	RIKEN cDNA 4930527E24 gene
10485711	−1.843	Fibin	fin bud initiation factor homolog (zebrafish)

10603986	−1.825	RP23-110D11.1	Xlr-related, meiosis regulated Xmr
10566810	−1.818	Nrip3	nuclear receptor interacting protein 3
10593123	−1.787	Tagln	Transgelin (Sm22)

The 20 most downregulated genes in E14.5 Tshz3 mutant ureters. Shown are fold change mutant (KO)/wild-type ureters. Several downregulated genes in *Tshz3* mutant ureters are genes usually induced during smooth muscle differentiation [calponin, *Myh11*, *Actg2*, *Acta2* (*Sma-alpha*), transgelin (*Sm22-alpha*)]. The downregulation of *Aqp1* (−2.15) is superior to *Sma* (−2.11) and *Sm22* (−1.78), the expression regulation of which by *Tshz3* has been previously shown by immunohistochemistry (Caubit et al., 2008). Fold change = –1(experimental/reference). Values represent average over three independent experiments. The results were quantile normalised with respect to the probe GC content using the RMA algorithm (GC content adjustment, RMA background correction and mean probe set summarisation). Transcripts either not expressed or expressed at very low levels were removed by a maximum expression cutoff <100. This data filtering resulted in 173,540 of 234,872 probe sets and 22,495 meta-probe sets. After normalisation, the arrays were checked for outliers using the principal component analysis with a correlation dispersion matrix and normalised Eigenvector scaling. No outliers were detected. Microarray probe sets representing transcripts changed by twofold or more were further analyzed. This data filtering resulted in 14,579 listed genes. Differential expression of summarised gene level expression was calculated using the Partek two-way ANOVA statistic followed by false discovery rate (FDR) multiple testing correction. Resulting *P*-values and FDR values indicated the probability of differential expression in state (wild type/knockout) and stage (embryonic stages 14 and 16). 2240 transcript clusters with an ANOVA FDR<0.05 in one of the conditions (genotype, stage, genotype*stage interaction) were defined as the significant differentially expressed subset.